MULTISCALE MODEL. SIMUL.
Vol. 8, No. 2, pp. 591–604

WIENER CHAOS EXPANSION AND SIMULATION OF ELECTROMAGNETIC WAVE PROPAGATION EXCITED BY A SPATIALLY INCOHERENT SOURCE*

MAJID BADIEIROSTAMI†, ALI ADIBI†, HAO-MIN ZHOU‡, AND SHUI-NEE CHOW‡

Abstract. First, we propose a new stochastic model for a spatially incoherent source in optical phenomena. The model naturally incorporates the incoherent property into the electromagnetic wave equation through a random source term. Then we propose a new numerical method based on Wiener chaos expansion (WCE) and apply it to solve the resulting stochastic wave equation. The main advantage of the WCE method is that it separates random and deterministic effects and allows the random effects to be factored out of the primary partial differential equation (PDE) very effectively. Therefore, the stochastic PDE is reduced to a set of deterministic PDEs for the coefficients of the WCE method which can be solved by conventional numerical algorithms. We solve these secondary deterministic PDEs by a finite-difference time domain (FDTD) method and demonstrate that the numerical computations based on the WCE method are considerably more efficient than the brute-force simulations. Moreover, the WCE approach does not require generation of random numbers and results in less computational errors compared to Monte Carlo simulations.

Key words. Helmholtz wave equation, stochastic differential equations, Wiener chaos expansion

AMS subject classifications. 60H15, 65C20, 35L05

DOI. 10.1137/090749219

1. Introduction.

In many optical phenomena in nature, the propagating light beam is diffuse and has some random fluctuations and uncertainties associated with it [1, 2]. Such a diffuse light beam can be originated from a spatially incoherent source like an incandescent lamp, or it might be a result of multiple scattering from different regions of a propagation environment. In either case, the light beam, which is inherently an electromagnetic wave, cannot be modeled by a deterministic field. To physically model such a diffuse (i.e., spatially incoherent) source, we normally use stochastic processes [3, 4]. Therefore, the resultant deriving equation will be a stochastic PDE in the form of the well-known electromagnetic wave equation. Unlike deterministic PDEs, solutions of stochastic PDEs are random fields. However, in most cases the physical evaluation is based on the statistical moments (e.g., mean, variance) of the solutions rather than the solutions themselves. Therefore, it is highly desired to be able to calculate these statistical moments independent of finding the random solutions.

The governing stochastic electromagnetic wave equation is usually too complex to be solved analytically; therefore numerical simulations play a significant role in solving this useful class of PDEs. So far, the most commonly used method in simulation of random effects modeled by a stochastic PDE is the Monte Carlo method. It solves the stochastic PDE for each realization of the random excitation and then finds desired statistical moments from the solutions. Although this technique is general and can be applied to a variety of PDEs under different scenarios, it has some major limitations.

*Received by the editors February 10, 2009; accepted for publication (in revised form) October 22, 2009; published electronically January 20, 2010.
http://www.siam.org/journals/mms/8-2/74921.html
†School of Electrical and Computer Engineering, Georgia Institute of Technology, Atlanta, GA 30332 (badiei@ece.gatech.edu, abibi@ece.gatech.edu).
‡School of Mathematics, Georgia Institute of Technology, Atlanta, GA 30332 (hmzhou@math.gatech.edu, chow@math.gatech.edu).

For instance, in order to correctly simulate a random effect, many realizations have to be computed to obtain a reliable estimate of various statistical properties. Its accuracy is merely controlled by the law of large numbers, which is rather slow in many problems. Moreover, in the Monte Carlo method we need a random number generator that naturally increases the numerical error and consequently degrades the accuracy of the solution.

In this paper, we propose to use a more efficient and accurate approach for realization of spatially incoherent light sources based on the Wiener chaos expansion (WCE) method, which has been widely used for many different problems for both analytical and numerical purposes [5, 6, 7, 8, 9, 10, 11, 12, 13, 14]. In this method, both the spatially incoherent source and the random solutions of the wave equation are expanded over independent standard Gaussian random variables. The WCE separates the deterministic effects from the randomness in the stochastic PDE. Consequently, it results in a system of deterministic PDEs for the expansion coefficients, which is referred to as its propagator [7]. The propagator is the mechanism responsible for the evolution of the randomness inherent to the original stochastic PDE. Remarkably, the propagator has the same form as the original equation. Once the propagator is determined, standard deterministic numerical methods can be applied to solve it efficiently. The main statistics (such as mean, covariance, and higher-order statistical moments) can be calculated by simple formulas involving only the coefficients of the propagator. In the WCE approach, there is no randomness directly involved in the computations. One does not have to rely on random number generators, and there is no need to solve the stochastic PDEs repeatedly over many realizations. Instead, the propagator system is solved only once.

Since the propagator is a set of deterministic PDEs for the WCE coefficients, any numerical simulation method can be used to solve it. Here we use the standard finite-difference time domain (FDTD) technique which is widely used to numerically simulate the electromagnetic wave equation [15]. Furthermore, we compare the results obtained using the WCE method to the results of the brute-force method, which is a direct simulation method based on the exact definition of a spatially incoherent source [3]. We will show that the WCE method very accurately resembles the results of the brute-force method at a much faster pace. We also use a photonic crystal (PC) structure [16], which is a typical inhomogeneous optical material for validation of our numerical simulations. Nevertheless, the model is not limited to PCs and can be applied to any other optical material.

In what follows, we first briefly introduce the WCE method and some of its significant properties in section 2. Then in section 3 we apply the WCE method to the electromagnetic wave equation (i.e., Helmholtz wave equation) driven by a spatially incoherent source, and we form its associated propagator. The propagator is then numerically solved by a standard FDTD technique for a typical PC structure as a propagation environment, and the results are compared to those of the brute-force simulations in section 4. Advantages and limitations of the proposed method are discussed in section 5. Final conclusions are made in section 6.

2. Wiener chaos expansion. As mentioned earlier in section 1, WCE has been intensively used for solving stochastic PDEs in many different fields. Here, we briefly introduce the expansion and emphasize some of its useful properties for linear equations. Let u be a solution of a linear stochastic PDE

$$L(u) = \sigma \dot{W}(x,t), \tag{2.1}$$

where L is a linear differential operator and $W(x,t)$ is a spatial-temporal Brownian motion. u is a function of x, t, and the Brownian motion. It would be beneficial if one could solve this equation by separating the deterministic spatial-temporal variables x and t from the random variable $W(x,t)$. At the beginning, this idea might appear to be impossible or at least impractical due to the infinite-dimensional nature of the Brownian motion $W(x,t)$. Nevertheless, the information contained in the path of a Brownian motion can be efficiently quantized.

To be more specific, let's take a temporal Brownian motion $W(t)$ as an example. For any orthonormal basis $\{m_i(s),\, i = 1,\, 2, \ldots\}$ in $L^2([0,t])$, define

$$\xi_i = \int_0^t m_i(s)dW(s), \quad i = 1,\, 2, \ldots. \tag{2.2}$$

It is easy to show that ξ_i are independent standard Gaussian ($N(0,\, 1)$) random variables. Then we have the expansion

$$W(s) = \int_0^t \chi_{[0,s]}(\tau)dW(\tau) = \sum_{i=1}^{\infty} \xi_i \int_0^s m_i(\tau)d\tau \tag{2.3}$$

for all $s \le t$, where $\chi_{[0,s]}(\tau)$ is the characteristic function of interval $[0, s]$. The expansion in (2.3) converges in the mean square sense,

$$E\left[W(s) - \sum_{i=1}^{N} \xi_i \int_0^s m_i(\tau)d\tau\right]^2 \to 0 \quad \text{as } N \to \infty,$$

with $E[.]$ representing the expected value of a random variable. For many choices of basis functions (e.g., Haar wavelets or trigonometric functions) the convergence in (2.3) holds with probability 1 and uniformly for $s \le t$.

For the choice of sinusoidal basis functions that will be used later in this paper,

$$\begin{cases} m_1(s) = \dfrac{1}{\sqrt{t}}, \\ m_i(s) = \sqrt{\dfrac{2}{t}} \cos\left((i-1)\pi \dfrac{s}{t}\right), \quad i = 2,\, 3, \ldots, \end{cases} \tag{2.4}$$

one can easily show that

$$\begin{aligned} E\left[W(s) - \sum_{i=1}^{N} \xi_i \int_0^s m_i(\tau)d\tau\right]^2 &= E\left[\sum_{i=N+1}^{\infty} \xi_i \int_0^s m_i(\tau)d\tau\right]^2 \\ &= \sum_{i=N+1}^{\infty} \left(\int_0^s m_i(\tau)d\tau\right)^2 \\ &\le C\frac{1}{N}, \end{aligned} \tag{2.5}$$

where C is a constant independent of N.

In the same way, one can derive a similar expression for $W(x)$ if a spatial Brownian motion is considered, and a simple tensor product can lead to the expression for a spatial-temporal Brownian motion,

$$W(x,t) = \sum_i \xi_i \int_0^x \int_0^t m_i(l,s)dlds, \tag{2.6}$$

where $\{m_i(l,s),\, i = 1,\, 2, \ldots\}$ form an orthonormal basis of $L^2([0,x] \times [0,t])$.

Replacing $W(x,t)$ in (2.1) by (2.6), we have

$$L(u) = \sigma \sum_i \xi_i m_i(x,t). \tag{2.7}$$

This indicates that the solution u is a function of x and t as well as the random variables ξ_i.

Using the fact that ξ_i are independent and L is a linear operator, we multiply (2.7) by ξ_i and take the expectation to obtain

$$L(u_i) = \sigma m_i(x,t), \tag{2.8}$$

where $u_i = E(u,\xi_i)$, and

$$u = \sum_i u_i \xi_i. \tag{2.9}$$

Equation (2.8) is the associated propagator of the primary stochastic PDE given in (2.1). Clearly, it has the same form as the stochastic PDE while it is absolutely deterministic. This is the most significant observation, which tells us that we can successfully factor out the random effects from the stochastic PDE. The expansion in (2.9) is the WCE of u for linear equations.

In the following section, we will apply the WCE method to the Helmholtz wave equation excited by a spatially incoherent source.

3. WCE method for stochastic Helmholtz wave equation. Most of the light sources used in practical applications (e.g., sensing) are spatially incoherent. Although there are numerous reports on the physical properties of an incoherent beam in the context of optical coherence theory [3], to the best of our knowledge there is no explicit report on the direct simulation of its propagation behavior inside an optical medium. In this section, we first propose a new stochastic model for spatially incoherent light sources which drives the electromagnetic wave equation and then apply the WCE method to rigorously solve it.

Figure 1 shows our simulation platform, which is composed of a planar inhomogeneous dielectric material as the propagation environment. The source line is placed in front of the propagation medium along line A, and the electric field values are monitored along the output line B. All the input sources are excited with a transverse

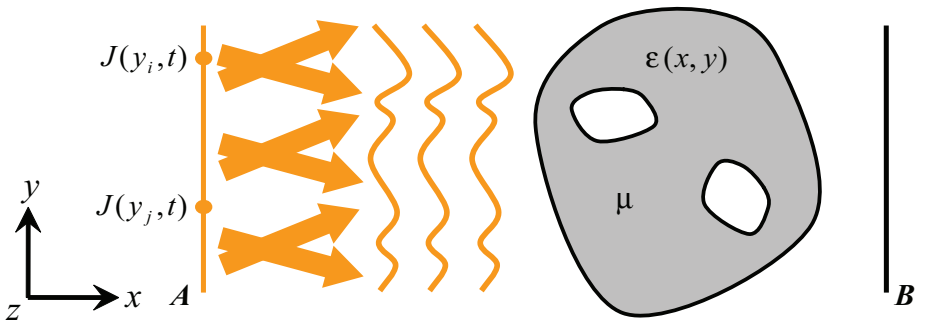

FIG. 1. *Propagation of a spatially incoherent source from the input source line A to the output line B in a typical environment is shown schematically.*

electric polarization (where the electric field is parallel to the z-axis). Due to the z-invariant nature of the setup, the electromagnetic wave propagation throughout the medium can be reduced to a two-dimensional (2D) Helmholtz wave equation,

$$\nabla^2 E_z(x,y,t) - \mu\varepsilon(x,y)\frac{\partial^2 E_z(x,y,t)}{\partial t^2} = \mu\frac{\partial J_z(x,y,t)}{\partial t}, \tag{3.1}$$

where the current density (J_z) is the source of excitation, and μ and $\epsilon(x,y)$ are the permeability and permittivity of the propagation environment, respectively. Here our source is modeled as a one-dimensional array of spatially incoherent point sources along line A. For modeling the spatially incoherent source, any two point sources on line A should radiate independently of each other. More specifically, the spatially incoherent source is defined as

$$\langle J_z^*(y_i,t)J_z(y_j,t)\rangle = \delta(y_i - y_j, t).$$

This definition by itself can be used as the brute-force technique for numerical modeling of the spatially incoherent source. In brute-force modeling, we enforce zero correlation between the contributions from every two input point sources by separately analyzing the structure with each point source and adding the individual contributions at the output line B incoherently (i.e., in power) [3].

Note that the input source along line A in Figure 1 is a deterministic function of time, and its stochastic nature is only in the spatial dimension (i.e., y in Figure 1). To model the spatially incoherent source, we use the white noise, i.e., the derivative of the Brownian motion, to model the spatial part of the current density (J_z). More precisely, we represent the spatially incoherent source along line A (i.e., $x = x_A$) as

$$J_z(y,t) = dW(y)V(t), \tag{3.2}$$

where $V(t)$ is a deterministic function representing the time variation of the source and $dW(y)$ is the derivative of the Brownian motion representing the independent spatial randomness along y. Note that assuming J_z to be a separable function of space (y) and time (t) is consistent with all practical applications in which the time variation of the source is assigned by the frequency range of operation and is usually the same at all points along the source line.

Following the formulation developed in section 2, by choosing any orthonormal basis functions ($m_i(s)$) in $L^2([0,y])$, we can expand $dW(y)$ as

$$dW(y) = \sum_i m_i(y)\xi_i, \tag{3.3}$$

where $\xi_i = \int_0^y m_i(s)dW(s), i = 1, 2, \ldots$.

Now both the input source (J_z) and the electric filed (E_z) are expanded using the WCE method similar to (2.9) as

$$J_z(y,t) = \sum_i m_i(y)V(t)\xi_i, \tag{3.4}$$

$$E_z(x,y,t) = \sum_i E_{zi}(x,y,t)\xi_i. \tag{3.5}$$

The expansion in (3.5) separates the deterministic effects ($E_{zi}(x,y,t)$) from the randomness (covered by ξ_i). By placing (3.4) and (3.5) into (3.1), the original stochastic

Helmholtz wave equation is reduced to its propagator, which is an associated set of decoupled deterministic equations for the expansion coefficients $(E_{zi}(x, y, t))$ as

$$\nabla^2 E_{zi}(x, y, t) - \mu\varepsilon(x, y)\frac{\partial^2 E_{zi}(x, y, t)}{\partial t^2} = \mu m_i(y)\frac{dV(t)}{dt}, \quad i = 1, 2, \ldots. \tag{3.6}$$

We summarize this observation into the following theorem.

THEOREM 3.1. *The solutions of the Helmholtz wave equation* (3.1) *excited by a spatially incoherent source must be Gaussian distributed and have the expression*

$$u\,(x, y, t, W(y)) = \sum_i u_i^m(x, y, t)\xi_i, \tag{3.7}$$

where $u_i^m(x, y, t)$ *are deterministic coefficients and* ξ_i *are independent standard Gaussian random variables constructed as* $\xi_i = \int_0^y m_i(s)dW(s), i = 1, 2, \ldots$.

It is worth mentioning that the linearity of the primary PDE in (3.1) makes the application of the WCE method much easier than its application for nonlinear PDEs. It can be shown that all the statistical moments of the random solution of the original stochastic PDE at the output line B in Figure 1 can be directly calculated using these expansion coefficients [14]. Obviously, by choosing the number of expansion coefficients considered in (3.3), the accuracy and the length of the simulation time can be varied. Fortunately, it is known that WCE is a very fast converging expansion technique, and usually does not require many expansion coefficients [5, 6, 8, 10, 11, 13]. Thus, by using only a few terms in (3.3), we can achieve enough accuracy in a very fast simulation for almost all practical optical structures.

4. Numerical simulation of spatially incoherent sources. Although the WCE technique is general and can be applied to any material system, the structure we consider here is a 2D photonic crystal (PC) as shown in Figure 2. It is composed of square lattice of cylindrical air holes etched in silicon. The radius of the air holes is $0.3a$, where a is the lattice constant (i.e., period). We fix the size of the PC structure with dimensions $x_f = 10a$ and $y_f = 20a$. For the wave propagation simulation, we use the standard FDTD method. The x-y plane is discretized so we get 24 grid cells per lattice constant (a) along both x- and y-axes. The source line A is placed in the air one lattice constant (i.e., 24 grid cells) before the interface of the PC structure, and the output line B is fixed 3 grid cells after the interface of the PC structure in the air. To minimize the nonphysical reflections from the computation boundary, a perfectly matched layer (PML) 12 grid cells wide [15] is set up around the structure. Note that all of these parameters for the PC geometry and for the simulation grid are chosen just to set an example and by no means affect the applicability or accuracy of our model.

4.1. Brute-force model. As we have already mentioned, one possible method to model a spatially incoherent source is to turn on one individual source at a time on the input line A, find the power spectrum due to each source at all points at the output line B, and then add these individual source contributions together incoherently (i.e., in power). While this technique models the incoherent source perfectly, it is very time consuming since it requires one simulation of the entire structure for each input point source along line A in Figure 2. Knowing that even a single numerical simulation of a PC structure with dimensions suitable for practical applications is very time consuming, the use of the brute-force method is not a practical option. We use this method only as a reference to assess the accuracy of our more efficient WCE method.

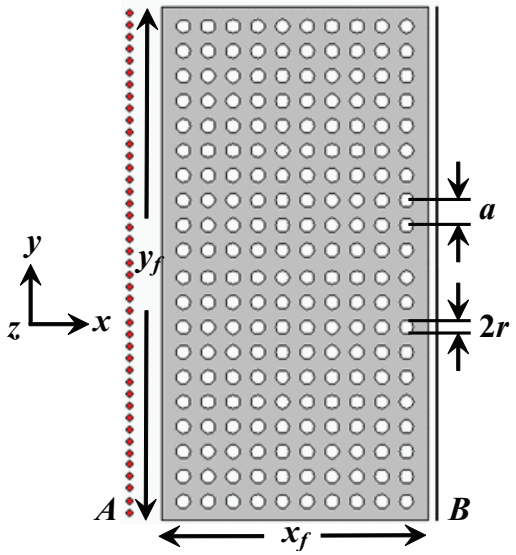

FIG. 2. *The schematic of a 2D square lattice PC structure of air holes in silicon with hole radius r and lattice constant a. The input (or source) and output lines are shown by A and B, respectively.*

In the numerical simulation of the brute-force method, one source is excited at a time with a commonly used sinusoidal modulated Gaussian pulse for the time function $V(t)$ [15],

$$V(t) = \sin\left(\omega(t - t_0)\right) \exp\left(-\left(\frac{t - t_0}{T}\right)^2\right), \tag{4.1}$$

to cover the desired range of frequencies. This pulse propagates all the way through the structure to get to the output line B. The normalized center frequency of the pulse (ω) is 0.04 and its width ($\Delta\omega$) is 0.016. The normalized width of the Gaussian pulse (T) in the time domain is $1/\Delta\omega = 62.5$, which corresponds to 120 time steps in our FDTD simulation. In order to find the steady state field profile at the output line B, we have to run the simulation for about 65000 time steps. Since we have assigned one point source to each grid cell along input line A, it adds up to $20 \times 24 = 480$ point sources (corresponding to $y_f = 20a$ and 24 grid cells per lattice constant, a), and this results in a total simulation time of 480×65000 time steps.

4.2. WCE model. Using the formulation described in section 3, we need to solve the set of deterministic PDEs given in (3.6) for the expansion coefficients $(E_{zi}(x, y, t))$. In this section, we numerically solve these deterministic PDEs using the FDTD technique. The deterministic time function (i.e., $V(t)$) and the stochastic spatial function (i.e., $dW(y)$) of the source are separated as shown in (3.2). For the numerical simulation of the WCE method, we use the sinusoidal modulated Gaussian pulse given in (4.1) for the time function. However, for the spatial part we choose a set of sinusoidal basis functions for $m_i(y)$ as given in (2.4). It is worth mentioning that in general we can choose any orthonormal basis for the spatial function ($dW(y)$ in (3.3)). The functions used here are primarily selected for their simplicity.

In the numerical simulations, we need to simulate the structure for each basis function $m_i(y)$ $(i = 1, 2, \ldots, M)$ to find the corresponding $E_{zi}(x, y, t)$ defined in (3.6)

at the output line B (i.e., $x = x_B$). In each simulation all the point sources along line A are excited simultaneously. However, the amplitude of the time function at each point source is modulated with the value of $m_i(y)$ at its corresponding vertical position. We can then calculate all statistical properties of the output field using its corresponding expansion coefficients. For example, prior to calculating the power spectrum of light at the output line B, we need to find the second moment [3] of the random field values in the frequency domain (i.e., $\langle E_z^2(x,y,\omega)\rangle_e$) from (3.1). This can be simply calculated by using the Fourier transform of its corresponding expansion coefficients ($E_{zi}(x,y,\omega)$) as

$$\langle E_z^2(x,y,\omega)\rangle_e = \sum_i |E_{zi}(x,y,\omega)|^2. \tag{4.2}$$

It should be noted that the Fourier transform is a linear transformation, and thus all formulations for the statistical moments in the time domain are kept unchanged in the frequency domain. The key advantage of the WCE technique is its fast convergence. With M expansion coefficients selected in (3.6), the total simulation time is M times the simulation time of the original structure with a deterministic input (i.e., $M \times 65000$ time steps).

5. Simulation results and discussion. The simulation result of the electric field power spectrum versus the normalized frequency at a typical point on the output line B is shown in Figure 3. For this simulation, we used only $M = 15$ expansion coefficients. The same data calculated using the brute-force technique are also shown in Figure 3 for comparison. The excellent agreement between the fast simulation using the WCE model and the long simulation using the brute-force model is visible from Figure 3. To calculate the gain in the simulation time using the WCE model, we just

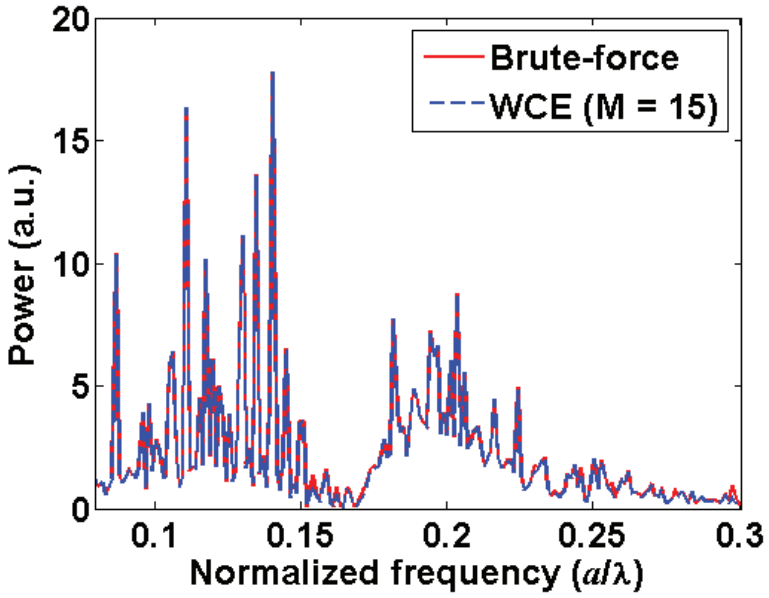

FIG. 3. *The electric field power spectrum as a function of normalized frequency at a typical point on the output line B in Figure 2 is shown. The simulation result of the WCE model was obtained with only $M = 15$ expansion coefficients.*

need to compare the total number of simulations of the entire structure needed in the two models. This number is equal to $M = 15$ (i.e., the number of the expansion coefficients) for the WCE model, while it is equal to the number of FDTD grid cells along the source line A, which is 480 for the brute-force model. Thus, the simulation based on the WCE model is 32 times faster than that using the brute-force model.

5.1. Comparison of the brute-force model and the WCE model. Figure 4(a) shows the relative error of the WCE model with respect to the brute-force model as a function of the number of expansion coefficients, M. To calculate the relative error, we first calculate the sum of the square of the differences between the two power spectra (from the two models) for all frequencies and all points at the output line B. Then we divide this sum by the sum of the square of the power spectrum for all frequencies and all points at the output line B calculated using the brute-force model. The exact mathematical formulation for the relative error is as follows:

$$Error = \frac{\sum_{i}^{N_p}\sum_{j}^{N_f}\left(\left\langle E^2_{zBF}(x_B, y_i, \omega_j)\right\rangle_e - \left\langle E^2_{zWCE}(x_B, y_i, \omega_j)\right\rangle_e\right)}{\sum_{i}^{N_p}\sum_{j}^{N_f}\left\langle E^2_{zBF}(x_B, y_i, \omega_j)\right\rangle_e},$$

where N_p and N_f are the number of grid cells on output line B and the number of discrete frequencies in our numerical simulation, respectively. Note that we use all the frequencies and all the points at the output line B to show the accuracy of our model. Figure 4(a) clearly shows that the results of the WCE model very quickly become close to those of the brute-force model with negligible error (the error is 0.08% for $M = 15$), which is a direct observation of its fast convergence.

Figure 4(b) shows the simulation time advantage of the WCE model with respect to the brute-force model. As seen in this figure, for larger M values the gain in simulation time of the WCE model over the brute-force model is decreased. This is because by increasing M, the number of distinct PDEs in (3.6) and equally the number of FDTD simulations for the WCE model are increased. Therefore, the overall WCE simulation takes longer. Table 1 shows the number of expansion coefficients M required in the WCE model for ensuring certain upper bounds of relative error. Correspondingly, the gain in simulation time is calculated and has been given in the table. As an example, for an accuracy better than 99%, we have to truncate the WCE series in (3.3) at $M = 12$, and hence the numerical simulation is performed almost 40 times faster than the brute-force model. Moreover, the data in Table 1 clearly verify the fast convergence behavior of the WCE model. Comparing the first and the third columns tells us by inclusion of only five more expansion coefficients in the WCE model that the error is reduced by 100 times.

5.2. Relation between the brute-force model and the WCE model. As the last comment in this section, we will show that there is a relation between the brute-force model and the WCE model.

Let $n_j(s)$ be another orthonormal basis for $L^2([0, y])$ too. Similar to the discussion given in section 2, we can construct $\eta_j = \int_0^y n_j(s)dW(s)$, and the solutions $u(x, y, t, W(y))$ have a different expression,

$$u(x, y, t, W(y)) = \sum_j u^n_j(x, y, t)\eta_j, \tag{5.1}$$

where $u^n_j(x, y, t)$ satisfies (3.6), with $m_i(y)$ being replaced by $n_j(y)$.

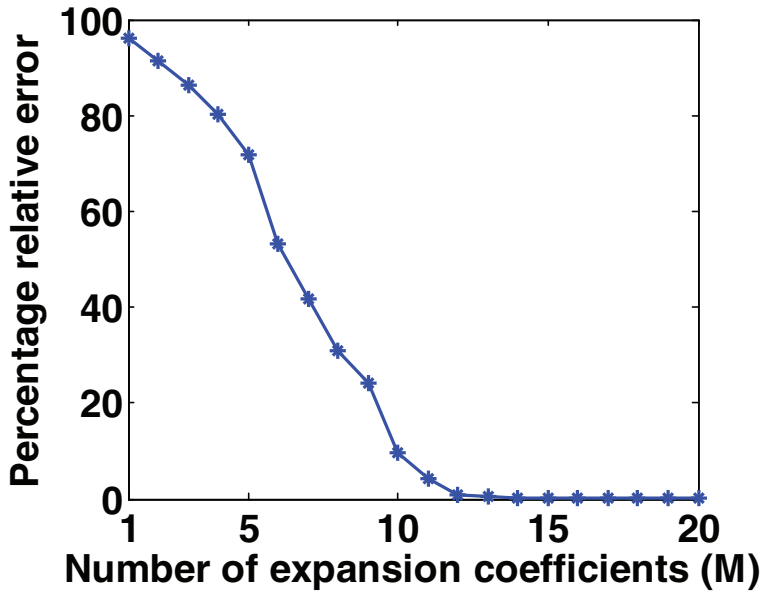

(a)

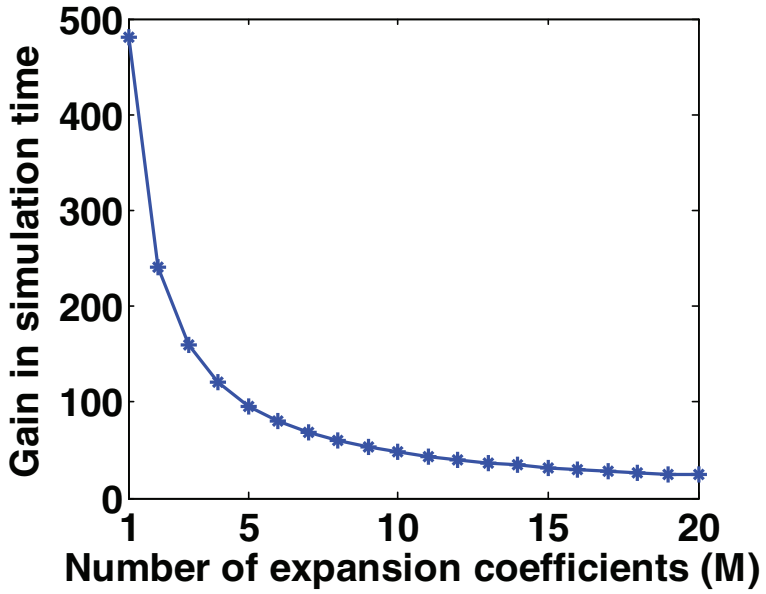

(b)

FIG. 4. (a) *The relative error and* (b) *the gain in the simulation time of the WCE model with respect to the brute-force model as a function of the number of expansion coefficients* (M).

TABLE 1
Number of expansion coefficients (M) *versus gain for a specific amount of relative error.*

Error	$< 10\%$	$< 1\%$	$< 0.1\%$
M	10	12	15
Gain	48	40	32

THEOREM 5.1. *The coefficients u_i^m and u_j^n satisfy the equation*

$$u_j^n = \sum_i \langle m_i, n_j \rangle u_i^m, \tag{5.2}$$

where $\langle m_i, n_j \rangle = \int_0^y m_i(s) n_j(s) ds$.

Proof. Since both $m_i(s)$ and $n_j(s)$ are orthonormal bases of $L^2([0, y])$, we must have

$$m_i(s) = \sum_j \langle m_i, n_j \rangle n_j(s).$$

Therefore, if we integrate both sides against $dW(s)$ over $[0, y]$, we have

$$\begin{aligned} \xi_i = \int_0^y m_i(s) dW(s) &= \int_0^y \sum_j \langle m_i, n_j \rangle n_j(s) dW(s) \\ &= \sum_j \langle m_i, n_j \rangle \int_0^y n_j(s) dW(s) = \sum_j \langle m_i, n_j \rangle \eta_j. \end{aligned}$$

Then by using (5.1) to expand the solution u on these two bases, we have

$$\sum_j u_j^n \eta_j = \sum_i u_i^m \xi_i = \sum_i u_i^m \sum_j \langle m_i, n_j \rangle \eta_j = \sum_j \left(\sum_i \langle m_i, n_j \rangle u_i^m \right) \eta_j,$$

which implies (5.2). ∎

THEOREM 5.2. *The brute-force solutions u_j^p and the WCE solutions u_i^m are related by the formulas*

$$u_j^p = \sum_i m_i(y_j) u_i^m \tag{5.3}$$

and

$$u_i^m = \sum_j m_i(y_j) u_j^p. \tag{5.4}$$

Proof. First of all, we note that in the brute-force method if the point source at y_j is excited, then $J_z(x_A, y, t) = \delta_j(y) V(t)$ is the input source for (3.1), where

$$\delta_j(y) = \begin{cases} 1 & \text{if } y = y_j, \\ 0 & \text{otherwise.} \end{cases}$$

We define

$$n_j^h(y) = \begin{cases} \dfrac{1}{\sqrt{h}}, & y \in \left[y_j - \dfrac{h}{2}, y_j + \dfrac{h}{2} \right], \\ 0 & \text{elsewhere.} \end{cases} \qquad j = 1, \ldots, N,$$

where $h = y_f / N$.

Denote u_j^h as the solutions of (3.6), with $n_j^h(y)\sqrt{h}V(t)$ as the input, which satisfies $\lim_{h\to 0} n_j^h(y)\sqrt{h}V(t) = \delta(y_j)V(t)$. We have

$$\lim_{h\to 0} u_j^h = u_j^p.$$

Following the linearity of (3.6), it is easy to check that u_j^h can be expressed as

$$u_j^h = \sum_i \langle n_j^h, m_i\rangle u_i^m.$$

Taking h to 0, we obtain (5.3).

On the other hand, the piecewise constant functions u_j^h span a subspace of $L^2([0, y])$ as

$$R_h = \text{span}\left\{n_j^h(y),\, j = 1, \ldots, N\right\}.$$

It is obvious that

$$\lim_{h\to 0} R_h = L^2([0, y]),$$

which implies

$$\begin{aligned} m_i(y) &= \lim_{h\to 0} \sum_j \langle m_i, n_j^h\rangle n_j^h(y) \\ &= \lim_{h\to 0} \sum_j \frac{1}{\sqrt{h}} m_i(y_j) h n_j^h(y). \end{aligned}$$

Following the linearity of (3.6) again, we have

$$\begin{aligned} u_i^m &= \lim_{h\to 0} \sum_j \langle m_i, n_j^h\rangle u_j^h \\ &= \lim_{h\to 0} \sum_j \sqrt{h} n_j^h(y) m_i(y_j) u_j^h \\ &= \sum_j m_i(y_j) u_j^p, \end{aligned}$$

which is (5.4). ∎

As mentioned earlier in section 4.2, we are particularly interested in the second moment of the solutions in many applications, and it can be computed by the WCE coefficients as follows.

COROLLARY 5.3. *Let u_j^p be the brute-force solutions with a point source at y_j. Let u_i^m be the solutions of (3.6), with $J_z(x_A, y, t) = m_i(y)V(t)$ as the input source. Then the second moment of the solutions is preserved:*

$$\sum_j \left|u_j^p\right|^2 = \sum_i |u_i^m|^2. \tag{5.5}$$

Proof. From (5.3) and the orthonormal property of $m_i(y)$, one has

$$\begin{aligned}\sum_j \left|u_j^p\right|^2 &= \sum_j \left(\sum_{i,k} m_i(y_j)m_k(y_j)u_i^m u_k^m\right)\\ &= \sum_{i,k}\left(\sum_j m_i(y_j)m_k(y_j)\right)u_i^m u_k^m\\ &= \sum_i \left|u_i^m\right|^2.\end{aligned}$$

This result confirms the equivalence of the second moments of the brute-force model and the WCE model as shown in Figure 3. Note that in general this is not true for other statistical moments. Hence, for a correct comparison between their other moments, one has to use the linear transformations given in Theorem 5.2 to find the corresponding relation. □

6. Conclusion. We have proposed a stochastic model for spatially incoherent sources. Then we have successfully applied the WCE method to solve the Helmholtz wave equation excited by such an input source. Using this method, it has been shown that the stochastic wave equation is reduced to a set of deterministic PDEs for the expansion coefficients of the random fields. All the statistical moments of the field values can be directly calculated using these expansion coefficients.

We have used the standard FDTD technique to numerically simulate these deterministic PDEs for a typical inhomogeneous propagation environment: a 2D square lattice PC. We have compared the WCE method with the exact brute-force model and demonstrated its advantage and efficiency. It has been shown that the WCE method very accurately models the propagation of spatially incoherent source much faster than the brute-force model. This is a consequence of the extremely fast convergence behavior of the WCE series in which a very small number of expansion terms is fairly enough for achieving accurate modeling.

Finally, it has been shown that the brute-force model defined in the old texts of classical optics is related to the WCE model through a linear transformation. Naturally, by wisely choosing the basis functions we can benefit from the reduced simulation time while not sacrificing accuracy. Of course the next step in this study is to search for the optimal set of basis functions that guarantees faster simulation of the spatially incoherent source, which is out of the scope of this manuscript.

Although we did not show any three-dimensional (3D) simulation in this paper, all the analytical formulation and numerical implementation can likewise be carried out on a 3D propagation medium and with no difficulty. Moreover, the simulation time advantage of the WCE model will be even more profound for 3D structures with 2D source planes as the number of input source points needed for the brute-force simulation will be huge in this case.

REFERENCES

[1] A. G. Yodh and B. Chance, *Spectroscopy and imaging with diffusing light*, Phys. Today, 48 (1995), pp. 34–40.

[2] A. G. Yodh and D. A. Boas, *Functional imaging with diffusing light*, in Biomedical Photonics Handbook, Chapter 21, CRC Press, Boca Raton, FL, 2003.

[3] L. Mandel and E. Wolf, *Optical Coherence and Quantum Optics*, Cambridge University Press, Cambridge, UK, 1995.
[4] J. W. Goodman, *Statistical Optics*, Wiley Classics Library Edition, John Wiley, New York, 2000.
[5] R. G. Ghanem and P. D. Spanos, *Stochastic Finite Elements: A Spectral Approach*, Springer-Verlag, Berlin, 1991.
[6] H. G. Matthies and C. Bucher, *Finite elements for stochastic media problems*, Comput. Methods Appl. Mech. Engrg., 168 (1999), pp. 3–17.
[7] R. Mikulevicius and B. L. Rozovskii, *Stochastic Navier-Stokes equations. Propagation of chaos and statistical moments*, in Optimal Control and Partial Differential Equations, J. L. Menaldi, E. Rofmann, and A. Sulem, eds., IOS Press, Amsterdam, 2001, pp. 258–267.
[8] M. Jardak, C. H. Su, and G. E. Karniadakis, *Spectral polynomial chaos solutions of the stochastic advection equation*, J. Sci. Comput., 17 (2002), pp. 319–338.
[9] S. Sakamoto and R. Ghanem, *Polynomial chaos decomposition for the simulation of non-Gaussian non-stationary stochastic processes*, J. Engrg. Mech., 128 (2002), pp. 190–201.
[10] D. Xiu and G. E. Karniadakis, *The Wiener–Askey polynomial chaos for stochastic differential equations*, SIAM J. Sci. Comput., 24 (2002), pp. 619–644.
[11] D. Xiu and G. E. Karniadakis, *Modeling uncertainty in flow simulations via generalized polynomial chaos*, J. Comput. Phys., 187 (2003), pp. 137–167.
[12] D. Lucor and G. E. Karniadakis, *Adaptive generalized polynomial chaos for nonlinear random oscillators*, SIAM J. Sci. Comput., 26 (2004), pp. 720–735.
[13] D. Zhang and Z. Lu, *An efficient, high-order perturbation approach for flow in random porous media via Karhunen-Loeve and polynomial expansion*, J. Comput. Phys., 194 (2004), pp. 773–794.
[14] T. Y. Hou, W. Luo, B. Rozovskii, and H. Zhou, *Wiener chaos expansions and numerical solutions of randomly forced equations of fluid mechanics*, J. Comput. Phys., 216 (2006), pp. 687–706.
[15] A. Taflove and S. C. Hagness, *Computational Electrodynamics*, Artech House, Norwood, MA, 2000.
[16] J. D. Joannopoulos, R. D. Meade, and J. N. Winn, *Photonic Crystals: Molding the Flow of Light*, Princeton University Press, Princeton, NJ, 1995.